

PACS 61.30.Gd, 75.30.Hx, 77.84.Nh

## **Dielectric properties of nematic liquid crystals with Fe<sub>3</sub>O<sub>4</sub> nanoparticles in direct magnetic field**

**O.P. Gornitska<sup>1</sup>, A.V. Koval'chuk<sup>1,2</sup>, T.N. Koval'chuk<sup>3</sup>, P. Kopčanský<sup>4</sup>, M. Timko<sup>4</sup>, V. Zavisova<sup>4</sup>, M. Koneracká<sup>4</sup>, N. Tomašovičová<sup>4</sup>, J. Jاذzyn<sup>5</sup>, I.P. Studenyak<sup>6</sup>**

<sup>1</sup>*National Aviation University, Institute of Innovative Technologies*

*1, Cosmonaut Komarov str., 03058 Kyiv, Ukraine*

<sup>2</sup>*Institute of Physics, National Academy of Science of Ukraine, 46, prospect Nauky, 03028 Kyiv, Ukraine*

<sup>3</sup>*V. Lashkaryov Institute of Semiconductor Physics, National Academy of Science of Ukraine,*

*45, prospect Nauky, 03028 Kyiv, Ukraine*

<sup>4</sup>*Institute of Experimental Physics, Slovak Academy of Sciences, 47, Watsonova str., 04001 Kosice, Slovak Republic*

<sup>5</sup>*Institute of Molecular Physics, Polish Academy of Sciences, 16, Smoluchowskiego str., 60179 Poznan, Poland*

<sup>6</sup>*Uzhgorod National University, 46, Pidhirna str., 88000 Uzhgorod, Ukraine*

**Abstract.** Researched within the frequency range  $10^{-1}$ – $10^6$  Hz were dielectric properties of pure 6CHBT liquid crystals and 6CHBT ones with the impurity of Fe<sub>3</sub>O<sub>4</sub> nanoparticles that have the mean diameter 5 nm and weight concentration  $10^{-4}$  %. The study was performed without and under the influence of direct magnetic field with the induction 0.45 and 0.60 T. It has been shown that the magnetic field influences on the parameters of the near-electrode area of liquid crystal. In the case of liquid crystal with magnetic nanoparticles, the parameter changes caused by the magnetic field depend on the induction value.

**Keywords:** dielectric properties of liquid crystals, magnetic impurities, orientation of liquid crystals.

Manuscript received 14.03.09; accepted for publication 14.05.09; published online 30.06.09.

### **1. Introduction**

Using the liquid crystals (LC) is mainly determined by the possibility of substantial variation of their properties under the influence of weak fields. In most devices that were already elaborated and widely used (LC displays), the different types of electro-optical effects are used. To create the electric field in a LC cell, it is necessary to deposit the electrodes transparent in the visible spectrum onto the boundary surfaces. Using the electro-optical effects, one needs to take into account the influence of near-electrode processes [1, 2]. All these factors that may create substantial problems (one of the basic problems is increase of the electro-optical response time) would be avoided by the influence of magnetic field on LC.

Magneto-optical effects in LC are revealed and studied for a relative long time. Their practical usage is restrained because anisotropy of magnetic permittivity of LC is far less than that of the dielectric one. Therefore, the rotational motion of LC molecules can be carried out under the influence of sufficiently strong alternative magnetic fields (units, tens of T). Up to date, devices for

creation of these fields are realized only in laboratory conditions and are not used in practice for their rather high cost.

It is possible to substantially increase the LC magnetic anisotropy due to the introduction of magnetic impurities (basically ferric oxides). As shown in [3, 4], in these ferronematics, the magnetic field induction of the Fredericksz transition differs from that for pure LC. To control magnetic impurity behavior in LC, they have to show certain characteristics: (i) small and controlled sizes and form, (ii) do not chemically interact with the LC molecules, and (iii) comparatively (with the LC molecules) weakly interact with each other. Magnetic nanoparticles obey to all these requirements, the technology of their preparation was successfully developed for recent few years.

In Refs [3-9], studied was the influence of magnetic nanoparticles on the Fredericksz transitions under the action of either electric field or magnetic one or under the simultaneous action of these fields in ferronematics based on different LC. It should be noted that experimental investigations were carried out mainly

for those conditions (orientation of molecules in a cell, orientation of the electric and magnetic field relative to orientation of director), for which detailed theoretical calculations were obtained [10].

It is known that in the case for reorientation of molecules (Fredericksz effect), the initial stage of molecular rotational motion takes place in the near-electrode area of a sample [11, 12]. Therefore, the investigation of processes occurred here is enough important for understanding the features of the very Fredericksz effect.

As shown in Refs [13, 14], the dielectric spectroscopy is the effective method to research the parameter change in a near-electrode area. Therefore, the aim of this work is to study the dielectric spectra of LC with magnetic nanoparticles in the direct magnetic field. To study the particular initial stage of molecular rotational motion, the measurements were carried out under the influence of the electric and magnetic fields, the voltage and induction values of which were sufficiently less than those necessary for complete reorientation of molecules. It should be noted that such experimental studies have not been performed before.

## 2. Materials and methods

The synthesis of the spherical magnetic nanoparticles was based on coprecipitation of  $\text{Fe}^{2+}$  and  $\text{Fe}^{3+}$  salts by  $\text{NH}_4\text{OH}$ . To obtain a  $\text{Fe}_3\text{O}_4$  precipitate,  $\text{FeSO}_4 \cdot 7\text{H}_2\text{O}$  and  $\text{FeCl}_3 \cdot 6\text{H}_2\text{O}$  were dissolved in deionized water by vigorous stirring (the ratio  $\text{Fe}^{3+}:\text{Fe}^{2+}$  was 2:1). The solution was heated to  $60^\circ\text{C}$  and 25%  $\text{NH}_4\text{OH}$  was added. The precipitate was isolated from solution by magnetic decantation and washing with water. Particles were coated with oleic acid as a surfactant at  $80^\circ\text{C}$ .

The magnetic properties were estimated by magnetization measurements using a vibrating sample magnetometer (Fig. 1), the saturation magnetization was 65 mT. Size and morphology of the particles were determined by transmission electron microscopy (TEM) (Fig. 2). The mean diameter of the magnetic nanoparticles was 4.8 nm (obtained by TEM). A histogram of the size distribution of the spherical magnetic particles is shown in Fig. 3.

The studied ferronematic samples were based on the thermotropic nematic 4-(trans-4'-n-hexylcyclohexyl)-isothiocyanatobenzene (6CHBT). 6CHBT is a low-melting enantiotropic liquid crystal with high chemical stability [15]. The temperature of the nematic-to-isotropic transition (clearing point) of the studied nematic is  $T_{NI} = 42.8^\circ\text{C}$ . The nematic samples were doped with a magnetic suspension that consists of nearly spherical  $\text{Fe}_3\text{O}_4$  magnetic particles coated with oleic acid as a surfactant. The doping was simply made by adding this suspension, under continuous stirring, to the liquid crystal in the isotropic phase. Due to the small volume concentrations of the magnetic particles ( $\sim 10^{-4}$ ) and surfactant in the prepared ferronematic samples, the interparticle dipole-dipole interactions are avoided.

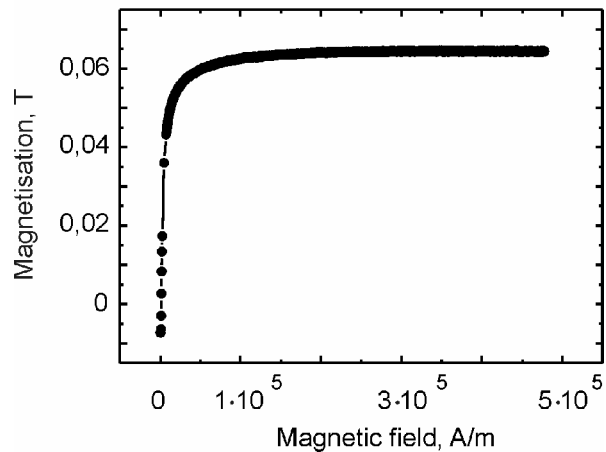


Fig. 1. Magnetization curve of prepared magnetic paste.

Frequency dependences of resistance  $R$  and capacity  $C$  were measured by using the oscilloscopic method [2, 16] under condition that the equivalent scheme of sample is the parallel linked resistance and capacity. The measuring signal had a triangular form; the amplitude was 0.25 V. The frequency of the measuring signal was changing within the range  $5 \cdot 10^{-2}$ – $10^5$  Hz.

Based on the known  $R$  and  $C$ ,  $\varepsilon'$  and  $\varepsilon''$  were determined. The direct magnetic field was created by two or four SaCo magnets that were located on both sides of glass substrates that bound the liquid crystal. In this case, the magnetic field was aligned with the electric one. The distance between the magnets is equal to the thickness of the measuring device cell, the area of magnets many times exceeded the square of electrodes, suggesting that the magnetic field in a sample is homogeneous. The magnetic field induction was measured by the calibrated Hall sensor. Dielectric properties of the samples were measured at the temperature 293 K.

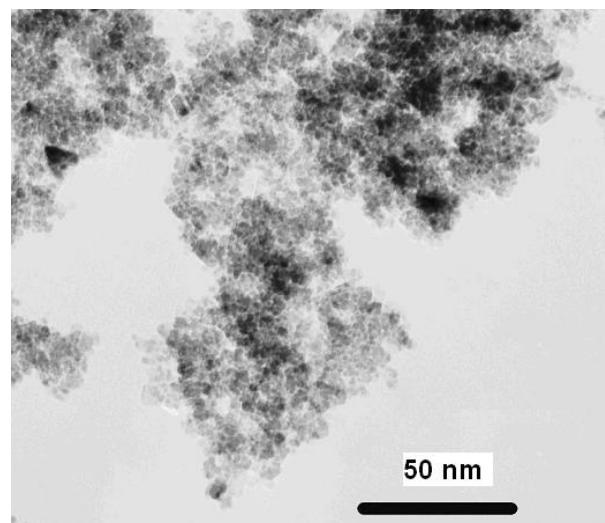
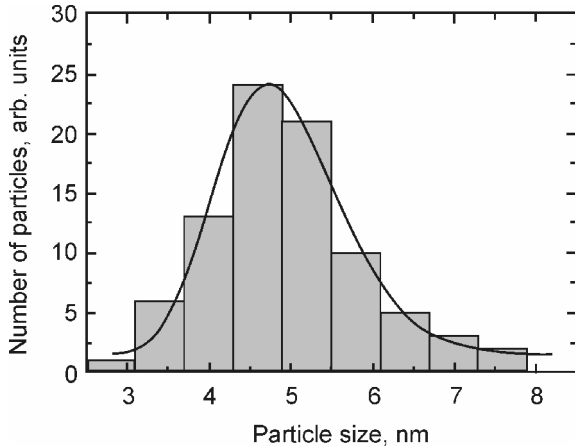


Fig. 2. TEM image of magnetic particles.



**Fig. 3.** Histogram of size distribution for spherical magnetic particles.

### 3. Experimental results and discussions

#### 3.1. Dielectric properties of pure LC

Fig. 4 presents the frequency dependences  $\varepsilon'(1)$  and  $\varepsilon''(2)$  of the planar oriented pure 6CHBT. The analysis of dielectric spectrum gives grounds to divide it into two parts: the part A ( $f < 10$  Hz) where substantial dispersion of complex dielectric permittivity components is observed, and the part B ( $f > 10$  Hz) where  $\varepsilon'$  is frequency independent and  $\varepsilon''$  decreases linearly with increasing the frequency (a sample resistance is frequency independent). As was shown in [2], the part B relates to those frequencies when near-electrode processes do not influence on the sample parameters (the electric field in a sample is homogeneous). Parameters determined in this part characterize the bulk properties of LC:  $\varepsilon'$  – the bulk dielectric permittivity  $\varepsilon_V$ , and  $\varepsilon''$  – the conductivity  $\sigma_{AC}$ . The  $\sigma_{AC}$  value was determined as follows:

$$\sigma_{AC} = \varepsilon_0 \varepsilon'' \omega, \quad (1)$$

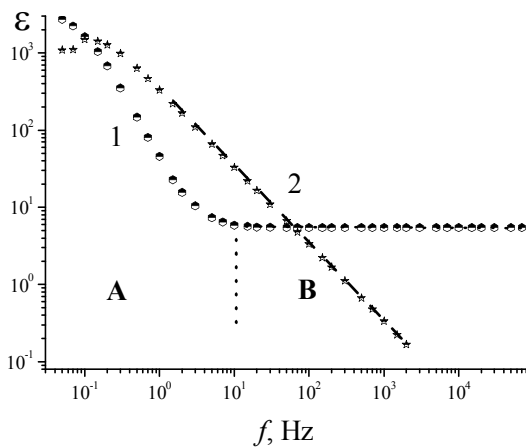


**Fig. 4.** Frequency dependences of  $\varepsilon'(1)$  and  $\varepsilon''(2)$  for planar-oriented 6CHBT at the temperature 293 K; thickness of the sample is 20  $\mu\text{m}$ .

**Table.**

Sample	<b>B, T</b>	$\sigma_{AC}$ , S/m	$\varepsilon_V$	$W$ , nm	$\tau$ , s
6CHBT	0	$1.9 \cdot 10^{-8}$	5.5	18	1.0
6CHBT	0.45	$1.8 \cdot 10^{-8}$	5.8	21	1.5
6CHBT	0.60	$1.9 \cdot 10^{-8}$	5.8	21	1.4
6CHBT+Fe <sub>3</sub> O <sub>4</sub>	0	$1.9 \cdot 10^{-8}$	6.1	21	1.6
6CHBT+Fe <sub>3</sub> O <sub>4</sub>	0.45	$1.9 \cdot 10^{-8}$	6.6	24	1.8
6CHBT+Fe <sub>3</sub> O <sub>4</sub>	0.60	$2.1 \cdot 10^{-8}$	6.6	25	1.8

where  $\varepsilon_0$  is the dielectric constant, and  $\omega = 2\pi f$  is the cyclic frequency. The estimated values of  $\varepsilon_V$  and  $\sigma_{AC}$  are summarized in Table. A comparison of the obtained  $\sigma_{AC}$  value for 6CHBT with the parameters for the other LC shows sufficiently high purity of the LC material under study.

The part B describes the initial stage of near-electrode processes. As was shown in [17, 18], the planar-oriented LC with positive anisotropy of dielectric permittivity is characterized by a relaxation process caused by dipole polarization in the near-electrode area of the sample. At the same time, in the very near-electrode area of a sample, a current is mainly provided by the rotational motion of dipoles within the range of angles equal to a fluctuation of the order parameter, and in the bulk – by ion transport. Our investigations of this relaxation process showed [17] that the dependence  $\varepsilon''(\varepsilon')$  (known as the Cole-Cole diagram) must be approximated by a semicircle. Similarly to dipole relaxation in the sample bulk, theoretically such relaxation process is described by the Debye equation:

$$\varepsilon^* = \varepsilon_\infty + \frac{\varepsilon_s - \varepsilon_\infty}{1 + i\omega\tau}, \quad (2)$$

where  $\varepsilon^*$  is the complex dielectric permittivity,  $\varepsilon_s$  and  $\varepsilon_\infty$  are the dielectric permittivities for the frequencies  $f = 0$  and  $f = \infty$ , accordingly,  $\tau$  is the time of dielectric relaxation.

Analysis of the Cole-Cole diagrams for the samples obtained without and under the influence of the magnetic field showed that these diagrams are described by the equation (2) with an experimental error that does not exceed 5%. Thus, it is possible to consider that, at the initial stage of molecular reorientation, a linear electro-optical effect may be substantial in the near-electrode area of the sample. Different polar impurities and, in particular, magnetic nanoparticles can influence on the parameters of this process.

Among the basic parameters that characterize the Debye dispersion is the time of dielectric relaxation. As shown in Table, this time is equal to one second for pure LC without the magnetic field.

The difference between the relaxation process resulting from dipole polarization in the near-electrode area of a sample and that in the bulk of a sample is rather

high values of  $\epsilon'$  and  $\epsilon''$  in the former case. Fig. 4 shows that they exceed the value of  $10^3$  for the frequency  $f=10^{-1}$  Hz. As was shown in [2], it is caused by a heterogeneous distribution of the electric field in a sample. If to suppose that the parameters of near-electrode areas near each of the electrodes are identical (the capacitances of near-electrode areas are identical) and the dielectric permittivity of near-electrode area equals  $\epsilon_V$ , then using the sample maximal capacitance (obtained using the analysis of the Cole-Cole diagram) for this relaxation process, it is possible to estimate the thickness of a near-electrode area [2, 17]

$$W = \frac{d\epsilon_V}{2\epsilon_s} \quad (3)$$

The  $W$  value for pure LC is also listed in Table. It equals 18 nm and differs little by the order of value from the same parameter for other LCs [2, 17, 18].

### 3.2. Influence of the magnetic field on dielectric properties of LC

Fig. 5 shows frequency dependences of the ratio of dielectric permittivity for pure 6CHBT under the action of the magnetic field  $\epsilon_B$  to that without the magnetic field  $\epsilon_0$  for  $\epsilon'(1, 2)$ ,  $\epsilon''(3, 4)$  and different values of the induction of 0.45 T (1, 3) and 0.60 T (2, 4). When analyzing the dielectric spectrum for pure LC, we consider separately the changes for bulk and near-electrode areas of the sample.

Fig. 5 and Table show that the magnetic field results to insignificant decrease of  $\sigma_{AC}$  and increase of  $\epsilon_V$ . As the  $\sigma_{AC}$  changes were close to experimental errors, the reasons that could cause these changes were not analyzed. Changes of the  $\epsilon_V$  value under the influence of the magnetic field are attributable to the partial rotational motion of molecules. This rotational motion may be realized only within the range of angles that relate to

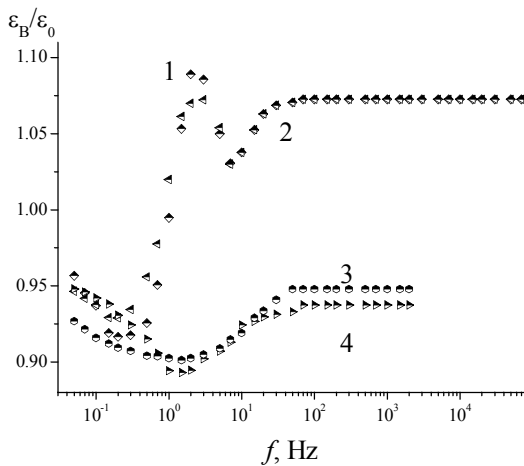


**Fig. 5.** Frequency dependences for the ratio of dielectric permittivity value for 6CHBT in the magnetic field  $\epsilon_B$  to that without the magnetic field  $\epsilon_0$  for  $\epsilon'(1, 2)$ ,  $\epsilon''(3, 4)$  and different values of the magnetic field induction 0.45 T (1, 3) and 0.60 T (2, 4) at the temperature 293 K.

fluctuations of the order parameter. Therefore, in practice the voltage for the Fredericksz effect could not have a threshold value. It is precisely this fact that explains that the changes under the magnetic field are identical for two different  $B$  values. It should be noted that the  $\epsilon_B/\epsilon_0$  ratio for the part A does not depend on the frequency (Fig. 5). And vice versa, for the part B the dispersion of the  $\epsilon_B/\epsilon_0$  ratio is observed, moreover, the frequency dependences of  $\epsilon_B'/\epsilon_0'$  ratio differ essentially from those of  $\epsilon_B''/\epsilon_0''$  one. As follows from Fig. 5, the  $\epsilon_B'/\epsilon_0'$  minimum value equals 0.92 at the frequency close to 0.3 Hz, and its maximal value equals 1.08 at  $f \approx 3$  Hz. At the same time, the  $\epsilon_B''/\epsilon_0''$  ratio has only a minimum value 0.9 at the frequency 2 Hz. It is also significant that, for pure LC, the  $\epsilon_B/\epsilon_0$  ratio and parameters of bulk part of the sample do not depend substantially on the value of the magnetic field induction.

As for the characteristics of the near-electrode relaxation process, the magnetic field results in the increase of the dielectric relaxation time and thickness of the near-electrode area (Table). It should be noted that the change of these parameters does not substantially depend on the value of the magnetic field, too.

### 3.3. Influence of magnetic nanoparticles on dielectric properties of LC

Fig. 6 presents the frequency dependences of ratio of the dielectric permittivity value for LC with magnetic nanoparticles  $\epsilon_{LM}$  to that for pure 6CHBT  $\epsilon_L$  at  $B = 0$ . From Table we see that presence of the magnetic particles does not influence on the  $\sigma_{AC}$  value but cause the increase of the  $\epsilon_V$  value. Invariability of the  $\sigma_{AC}$  value when introducing the magnetic nanoparticles suggests that these impurities were rather “pure” and did not influence on the concentration of charge carriers in LC. This fact is reasonably important for the analysis of the obtained results.

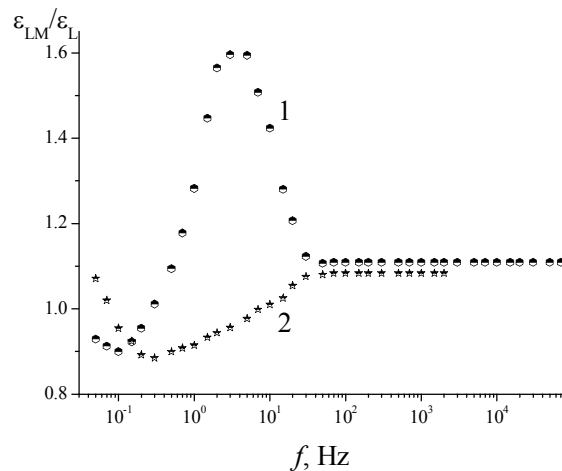


**Fig. 6.** Frequency dependences for the ratio of dielectric permittivity value for LC with magnetic nanoparticles  $\epsilon_{LM}$  to that for pure LC  $\epsilon_L$  at the temperature 293 K. The induction of magnetic field is  $B = 0$ ; thickness of the sample is 20  $\mu\text{m}$ .

The increase of dielectric permittivity when introducing the magnetic nanoparticles can be explained by two factors: (i) a rather high value of the dielectric permittivity of nanoparticles and (ii) a partial change in molecular orientation of LC [19]. Taking into account that a concentration of magnetic nanoparticles was rather small ( $10^{-4}\%$ ), the change of dielectric permittivity value of LC due to the implanted impurities is determined as follows

$$\Delta\varepsilon = 3c\varepsilon_V \frac{\varepsilon_M - \varepsilon_V}{\varepsilon_M + 3\varepsilon_V}, \quad (4)$$

where  $c = 10^{-4}\%$  is the concentration of magnetic nanoparticles,  $\varepsilon_M$  is the dielectric permittivity of magnetic nanoparticles.

When  $\Delta\varepsilon = 0.6$ , from the equation (4) it follows that this change can be caused by nanoparticles with a negative value of dielectric permittivity. It does not conform to the properties of the nanoparticles in any way. Therefore, the most probable explanation for the dielectric permittivity change due to  $\text{Fe}_3\text{O}_4$  nanoparticles can be influence of these nanoparticles on the pretilt angle of LC molecules.

As in the case of the magnetic field influence on properties of pure LC, the frequency dispersion of  $\varepsilon_{LM}/\varepsilon_L$  ratio for the part B differs for dielectric permittivity of each component. If the  $\varepsilon_{LM}'/\varepsilon_L'$  ratio has the maximum value (1.6) at 5 Hz and minimum one (0.9) at  $10^{-1}$  Hz, the  $\varepsilon_{LM}''/\varepsilon_L''$  ratio has the only minimum value (0.85) at frequency 0.3 Hz.

The presence of magnetic nanoparticles causes changes in parameters of the near-electrode relaxation process. As seen from Table, implantation of  $\text{Fe}_3\text{O}_4$  nanoparticles into LC results in increasing the relaxation time and thickness of the near-electrode area. Taking into account Ref. [18], it is possible to suppose that the relaxation time increase is a result of increase in the energy of adhesion of LC molecules to substrate. The influence of magnetic nanoparticles on the value of adhesion energy of LC molecules to substrate was studied in detail in Ref. [7].

### 3.4. Influence of the magnetic field on dielectric properties of LC with magnetic nanoparticles

Fig. 7 shows the frequency dependences of the ratio of dielectric permittivity for 6CHBT with  $\text{Fe}_3\text{O}_4$  nanoparticles under the influence of magnetic field  $\varepsilon_B$  to that without magnetic field  $\varepsilon_0$  for  $\varepsilon'$  (1, 2),  $\varepsilon''$ (3, 4) and different values of the magnetic field induction 0.45 T (1, 3) and 0.60 T (2, 4).

Like to the case of pure LC, the magnetic field increases the  $\varepsilon_V$  value. The  $\varepsilon_V$  variation for two values of the magnetic field induction does not depend on the  $B$  value within the range of experimental errors. Therefore, the results of magnetic field influence on the  $\varepsilon_V$  value for 6CHBT with  $\text{Fe}_3\text{O}_4$  nanoparticles and pure 6CHBT are not distinguished. As for the  $\sigma_{AC}$  value, it depends on the value of the magnetic field (Table), most probably the

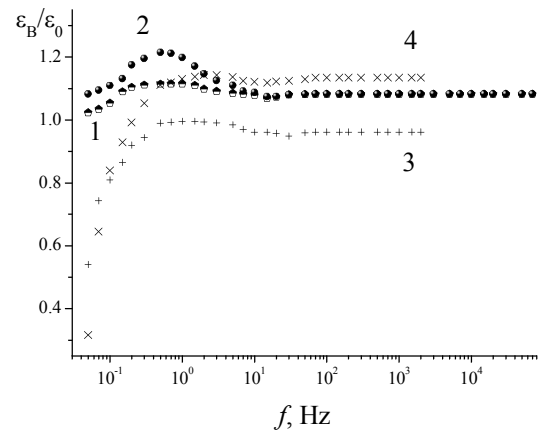


**Fig. 7.** Frequency dependences for the ratio of dielectric permittivity value  $\varepsilon_B$  for 6CHBT with  $\text{Fe}_3\text{O}_4$  nanoparticles in the magnetic field to that without the magnetic field  $\varepsilon_0$  for  $\varepsilon'$ (1, 2),  $\varepsilon''$ (3, 4) and different values of the magnetic field induction 0.45 T (1, 3) and 0.60 T (2, 4) at the temperature 293 K.

reason of this is a change of bulk properties of LC and, in particular, mobility of charge carriers.

The most cardinal differences between the dielectric spectra of  $\varepsilon_B/\varepsilon_0$  ratio for 6CHBT with  $\text{Fe}_3\text{O}_4$  nanoparticles and pure 6CHBT are observed for the part B. Unlike the frequency dependence of  $\varepsilon_B'/\varepsilon_0'$  ratio for pure 6CHBT, the similar frequency dependence for LC with nanoparticles has only one maximum value at the frequency close to 0.4 Hz. It is also significant that this particular maximal value (unlike for pure LC) depends on the value of the magnetic field.

A comparison of Figs 5 and 7 suggests that for the part B the  $\varepsilon_B''/\varepsilon_0''$  ratios for LC with nanoparticles and for pure LC differ substantially, too. Unlike the pure LC, the  $\varepsilon_B''/\varepsilon_0''$  ratio for LC with nanoparticles has a low maximum value at  $f \approx 1$  Hz, and then observed is the sharp drop in this value with frequency decreasing. It is also significant that the value of  $\varepsilon_B''/\varepsilon_0''$  ratio depends on the magnetic field value.

The analysis of parameters inherent to the near-electrode relaxation process shows that, like to the case of pure LC, the influence of magnetic field on LC with nanoparticles results in the increase of the relaxation time and thickness of near-electrode layer. Thus, it is important to note that the thickness of the near-electrode area depends on the induction.

## 4. Conclusions

1. The method of dielectric spectroscopy is rather effective to analyze the influence of nanoparticles at the initial stage of the Fredericksz effect in the magnetic or/and electric fields.

2. From the analysis of the frequency dependence of ratio of the dielectric permittivity for LC with

magnetic nanoparticles  $\varepsilon_{LM}$  to that for pure LC  $\varepsilon_L$ , it is possible to find those frequencies, at which the changes of parameters of the materials under study are maximal. These frequencies relate to the part of dielectric spectrum caused by near-electrode processes.

3. The low-frequency relaxation process is caused by dipole polarization of molecules in the near-electrode area and described by the Debye equation. The relaxation time (units of seconds) and thickness of the near-electrode area (tens of nanometers) were estimated. It has been shown that these parameters are increased when implanting the magnetic nanoparticles into LC and under the action of the magnetic field. In the case of LC with nanoparticles, the thickness of near-electrode area depends on the induction value.

4. Both for pure LC and LC with magnetic nanoparticles, the magnetic field more substantially influences on the parameters of near-electrode area than on bulk properties of samples. The ratios of the dielectric permittivity values under the magnetic field to that without the magnetic field are non-monotonous functions of frequencies, which relate to the near-electrode relaxation process. The frequency dependences of these ratios differ essentially for pure LC and LC with magnetic nanoparticles.

5. The ratio of the dielectric permittivity values under the magnetic field to that without the magnetic field in a greater measure depends on the magnetic field induction in the case of LC with nanoparticles than in the case of pure LC. It gives grounds to develop new materials for the indicators of the magnetic field.

#### Acknowledgements

This work was supported by the Slovak Academy of Sciences, in the framework of CEX-NANOFLUID, the project SAV-FM-EHP-2008-01-01, MNT-ERA Net 2008-022-SK, the projects VEGA 0077, APVV 0173-06, 0509-07 and Ministry of Education Agency for Structural Funds of EU in the frame of the project 26220120021.

#### References

1. G. Barbero, D. Olivero, Ions and nematic surface energy: Beyond the exponential approximation for the electric field of ionic origin // *Phys. Rev. E* **65**(3), 031701(2002).
2. A.V. Koval'chuk, Low-frequency spectroscopy as an investigation method of the electrode-liquid interface // *Functional Materials* **5**(3), p. 426-430 (1998).
3. P. Kopčanský, M. Koneracká, V. Zavisova et al., Study of magnetic Fredericksz transition in ferro-nematics. Liquid crystals doped with fine magnetic particles // *J. Phys. IV (Paris)* **7**, p. 565-566 (1997).
4. O. Buluy, E. Ouskova, Yu. Reznikov et al., Magnetically induced alignment of FNS // *J. Magn. Mater.* **252**, p. 159-161 (2002).
5. P. Kopčanský, N. Tomašovičová, M. Koneracká et al., Structural changes in the 6CHBT liquid crystal doped with spherical, rodlike, and chainlike magnetic particles // *Phys. Rev E* **78**(1), 011702 (2008).
6. P. Kopčanský, I. Potočova, M. Timko et al., The structural transitions in ferro-nematics in combined electric and magnetic fields // *J. Magn. Mater.* **272-276**, p. 2355-2356 (2004).
7. P. Kopčanský, I. Potočova, M. Koneracká et al., The anchoring of nematic molecules on magnetic particles in some types of ferro-nematics // *J. Magn. Mater.* **289**, p. 101-104 (2005).
8. P. Kopčanský, M. Koneracká, M. Timko et al., The structural transitions in ferro-nematics and ferro-nematic droplets // *J. Magn. Mater.* **300**, p. 75-78 (2006).
9. N. Tomašovičová, M. Koneracká, P. Kopčanský et al., The structural phase transitions in 6CB-based ferro-nematics // *Acta Phys. Pol. A* **115**(1), p. 336-338 (2009).
10. S.V. Burylov, Y.L. Raikher, Physics of ferro-nematics with soft particle anchoring // *Braz. J. Phys.* **25**(2), p. 148-173 (1995).
11. V. Boichuk, S. Kucheev, J. Parka et al., Surface-mediated light-controlled Fredericksz transition in a nematic liquid crystal cell // *J. Appl. Phys.* **90**(12), p. 5963-5967 (2001).
12. L.V. Mirantsev, Influence of substrate microrelief on the Fredericksz transition in a thin nematic cell // *Phys. Rev. E* **59**(5), p. 5549-5555 (1999).
13. A.V. Koval'chuk, Relaxation processes and charge transport across liquid crystal-electrode interface // *J. Phys.: Condens. Matter.* **13**(24), p. 10333-10345(2001).
14. A.V. Koval'chuk Low-frequency dielectric relaxation at the tunnel charge transfer across the liquid/electrode interface // *Functional Materials* **8**(4), p. 690-693 (2001).
15. R. Dabrowski, J. Dziaduszek, and T. Szczucinski // *Mol. Cryst. Liquid Cryst. Lett.* **102**, p. 155 (1984).
16. A.J. Twarowski, A.C. Albrecht, Depletion layer in organic films: Low frequency measurements in polycrystalline tetracene // *J. Chem. Phys.* **20**(5), p. 2255-2261 (1979).
17. A.V. Koval'chuk, Low and infra-low dielectric spectroscopy liquid crystal-solid state interface. Sliding layers // *Ukr. J. Phys.* **41**(10), p. 991-998 (1996).
18. O. Yaroshchuk, A. Kovalchuk, R. Kravchuk, The interfacial dipole-to-dipole interaction as a factor of polar anchoring in the cells with planar liquid crystal alignment // *Mol. Cryst. Liquid Cryst.* **438**, p. 195-204 (2005).
19. T. Gavrillo, O. Kovalchuk, V. Nazarenko et al., Orientational behaviour of a nematic liquid crystal filled with inorganic oxide nanoparticles // *Ukr. J. Phys.* **49**(12), p. 1167-1173 (2004).